LBNL-40127

ERNEST ORLANDO LAWRENCE
BERKELEY NATIONAL LABORATORY

Magnetic Detection of Ferrofluid Injection Zones

S.E. Borglin, G.J. Moridis, and A. Becker

Earth Sciences Division

March 1998

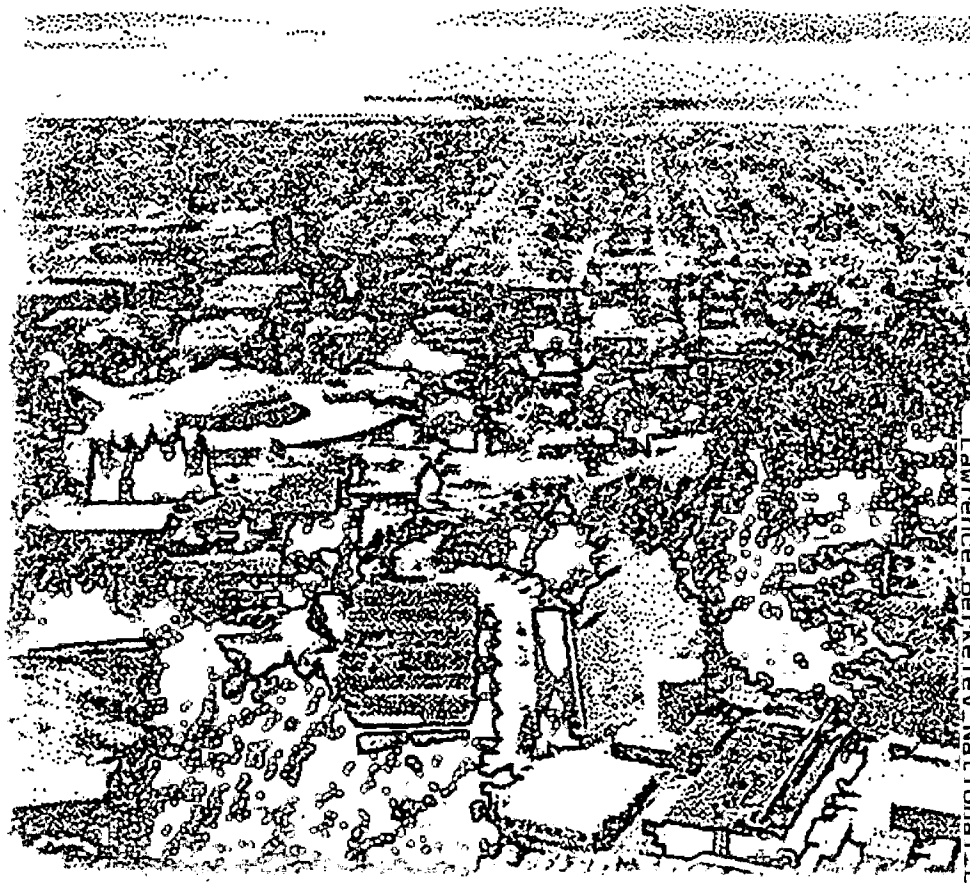

DISCLAIMER

LBNL-40127

MAGNETIC DETECTION OF FERROFLUID INJECTION ZONES

S.E. Borglin, G.J. Moridis and A. Becker

Earth Sciences Division
Lawrence Berkeley National Laboratory
Berkeley, CA 94720

March 1998

This work was supported by the Laboratory Directed Research and Development Program of Lawrence Berkeley National Laboratory under the U.S. Department of Energy, Contract No. DE-AC03-76SF00098.

Abstract

Ferrofluids are stable colloidal suspensions of magnetic particles that can be stabilized in various carrier liquids. In this study we investigate the potential of ferrofluids to trace the movement and position of liquids injected in the subsurface using geophysical methods. An ability to track and monitor the movement and position of injected liquids is essential in assessing the effectiveness of the delivery system and the success of the process. Ferrofluids can also provide a significant detection and verification tool in containment technologies, where they can be injected with the barrier liquids to provide a strong signature allowing determination of the barrier geometry, extent, continuity and integrity. Finally, ferrofluids may have unique properties as tracers for detecting preferential flow features (such as fractures) in the subsurface, and thus allow the design of more effective remediation systems.

In this report we review the results of our investigation of the potential of ferrofluids to trace the movement and position of liquids injected in the subsurface using geophysical methods. We demonstrate the feasibility of using conventional magnetometry for detecting subsurface zones of injected ferrofluids used to trace liquids injected for remediation or barrier formation. The geometrical shapes considered were a sphere, a thin disk, a rectangular horizontal slab, and a cylinder. Simple calculations based on the principles of magnetometry are made to determine the detection depths of FTs. Experiments involving spherical, cylindrical and horizontal slabs show a very good agreement between predictions and measurements.

1. INTRODUCTION

This report summarizes work on the use of ferrofluids for the detection and imaging of liquids in subsurface environmental applications conducted in Fiscal Year 1997 at the Lawrence Berkeley National Laboratory (LBNL). We investigate the potential of ferrofluids to to trace the movement and position of liquids injected in the subsurface using geophysical methods.

Ferrofluids represent a new development, and thus the existing body of information on their use in environmental and geophysical applications involving problems of flow and transport through porous media is very limited. To our knowledge, the only known study of the subject is currently in progress by this LBNL team [*Moridis et al.*, 1998; *Moridis and Oldenburg*, 1998;*Oldenburg et al.*, 1998; *Borglin and Moridis, 1998*].

1.1. Background

Ferrofluids are stable colloidal suspensions of magnetic particles in various carrier liquids [*Raj and Moskowitz*, 1990; *Ferrofluidics*, 1992]. The solid, magnetic, single-domain particles are small (with an average diameter of 3-15 nm) and are covered with a molecular layer of a dispersant. Thermal agitation due to Brownian motion keeps the particles suspended, while the dispersant coating prevents the particles from agglomeration. The stability of ferrofluids means that an external magnetic field does not lead to local changes in the concentration of the magnetic particles in the carrier liquid, i.e. the concentration of the

particles in the ferrofluid remains spatially and temporally constant regardless of the presence or strength of the external field. Consequently, ferrofluids behave like a homogeneous single-phase fluid when flowing under the influence of a magnetic field. This attribute is responsible for the unique property of ferrofluids that they can be manipulated in virtually any fashion, defying gravitational or viscous forces in response to external magnetic fields. Therefore, ferrofluids can be made to flow in a desired direction and move precisely without any physical contact [*Chorney and Mraz*, 1992].

Ferrofluids were first developed by NASA to handle liquid propellants in the absence of gravity in outer space. Due to their ability to be held in place by magnetic fields, they are currently used (a) in hermetic seal pumps, which eliminate leakage along rotating shafts and joints [*Bailey*, 1983], (b) as barriers against volatile organic compounds in chemical processing, (c) in rotating vacuum seals used in semiconductor processing and environmentally controlled chambers [*Moskowitz*, 1975], (d) in sealed microwave, laser, and nuclear applications [*Rosensweig*, 1979], as well as in computer disk drives. They are also used in niche areas such as high-fidelity audio speakers and precision bearings [*Chorney and Mraz*, 1992], and have a number of biomedical applications. Therapeutic agents have been incorporated into or onto the magnetic particles, which are then guided and concentrated by magnetic fields at specific body sites [*Senyei and Widder*, 1981; *Morimoto*, 1983). Ferrofluids have also been used as tracers of blood flow in non-invasive circulatory measurements [*Newbower*, 1972].

1.2. Significance and Applications

The ferrofluid-based environmental engineering approaches and applications investigated in this project are applicable to all sites in the DOE complex that involve the injection and monitoring of environmental liquids into the subsurface as a part of a remediation effort, and cover all the problem areas covered by the Focus Groups, i.e. High Level Waste Tanks, Mixed Waste, Subsurface Contamination, and Cross-Cutting Technologies. In particular, sites with pressing remediation needs and challenging conditions, such as Hanford, Savannah River, Oakridge, INEL and Fernald, could potentially benefit from the application of ferrofluids-based technologies.

Ferrofluids have several unique properties. They move as a homogeneous single-phase fluid under the influence of a magnetic field, with no separate consideration for the magnetic particles and the carrier liquid. They can be manipulated in virtually any fashion, defying gravitational or viscous forces in response to external magnetic fields [*Chorney and Mraz*, 1992]. Additionally, the magnetic particles cast a strong magnetic signature, which can be exploited for tracking injected liquids using geophysical methods.

The controlled emplacement of liquid reactants in order to treat or contain contaminants

in the subsurface is a critical problem in all aspects of *in-situ* remediation or containment, and its failure invariably leads to failure of the remediation method, regardless of its other merits or elegance. Current emplacement practices for subsurface treatment consist entirely of injection, and the mechanism for fluid guidance is pressure (potential) differentials. This is a 'brute-force' approach, often inefficient and unpredictable, because it is diffusive and subject to short-circuiting by highly-permeable zones. The ferrofluid-based approach proposed here can alleviate the adverse effects of heterogeneity and can lead to more accurate and effective technologies for targeting and delivery of reactants or other liquids to contaminated zones in the subsurface.

An ability to track and monitor the movement and position of injected liquids is essential in assessing the effectiveness of the delivery system and the success of the process. A number of geophysical methods (such as ground-penetrating radar, electrical resistance tomography, tiltmeters, etc.) can be used to accomplish this task. Ferrofluid tracers can also provide a powerful means for tracking the movement and location of liquids in the subsurface, as well as providing a means for testing the integrity of subsurface barriers (i.e. detection of holes). Ferrofluids used in conjunction with gelling barrier liquids may be useful as tracers to identify preferential and/or high-permeability pathways (along which the likelihood of contaminant migration is maximum) in the fractured rocks of the Yucca Mountain site.

1.3. Study Focus

In this report we discuss our investigation of the potential of ferrofluids to trace the movement and position of liquids injected in the subsurface using geophysical methods.

1.4. Ferrofluids for Monitoring, Verification and Tracing

A **F**errofluid for **T**racing and detecting liquids in the subsurface will be hereafter referred to as a FT. The magnetic particles cast a strong electromagnetic signature. Because of this property, ferrofluids are used commercially for magnetic pattern recognition in magnetic tapes, hard and floppy disks, crystalline and amorphous alloys, steels, and rocks [*Ferrofluidics*, 1992]. With a saturation magnetization M_{sat} in the $6,400$-$72,000$ A/m range (i.e., flux densities of 80-900 Gauss), this signature is sufficiently strong for magnetic detection methods at low loading volumes, i.e. 1-5%, which are insufficient to allow liquid movement in response to external fields. We propose to exploit this fact to develop a real-time monitoring of fluid movement and position during injection using **E**lectro**M**agnetic (EM) methods. Ferrofluids can also provide a significant detection and verification tool in

containment technologies, where they can be injected with the barrier liquids to provide a strong signature allowing determination of the barrier geometry, extent, continuity and integrity. Finally, ferrofluids may have unique properties as tracers for detecting preferential flow features (such as fractures) in the subsurface, and thus allow the design of more effective remediation systems.

1.4. Ferrofluid Properties

Ferrofluids have low viscosities (as low as 2 cp), thus allowing easy injection into the subsurface. Their small particle size (3-15 nm) minimizes potential filtration problems. Typical ferrofluids contain 10^{23} particles/m^3 and are opaque to visible light. They also possess a very high saturation magnetization. In magnetite-based ferrofluids the saturation magnetization M_{sat} varies between 6400-72000 A/m (flux densities of 80-900 Gauss). Neodymium -Iron-Boron and Samarium-Cobalt ferrofluids exhibit saturation magnetization about three times larger than similar magnetite systems. The size of the magnetic particles is limited by the stability requirements necessary to counter the magnetic field gradient, the gravitational field, and magnetic agglomeration. At a temperature of 25 ^oC it can be shown that the maximum size for stability is about 10 nm [*Rosensweig*, 1985]. Use of appropriate surfactants makes possible the stability of ferrofluids with larger particle sizes.

The algebraic sum of the van der Waals attractive energy, magnetic attractive energy, and steric repulsion energy (due to the presence of polar molecules adsorbed on the particle surface) determines the stable monodispersity of the particle suspensions in ferrofluids. The dispersant molecules can be polar surfactants with a polar head group attached to a long chain or long polymer molecules containing polar groups along the length of the chain and exhibiting multisite adsorption on the magnetic particle. Ferrofluids with several polar adsorbing groups (e.g. carboxyl, phosphate, sulfosuccinate, etc.) are available.

There is no long-range order between the particles of a colloidal ferrofluid. In the absence of a magnetic field, the particles are randomly oriented, and the fluid has no net magnetization. Ferrofluids are extremely *soft* magnetic materials, and as such do not exhibit hysteresis. The study of ferrofluids involves traditional ferromagnetic concepts. The relationship between the induction field $\vec{B}$, the external magnetic field $\vec{H}$ and the intensity of magnetization $\vec{M}$ of a ferrofluid is given by

$$\vec{B} = \mu_m(\vec{H} + \vec{M}), \tag{1.1}$$

where μ_m is the magnetic permeability. The effect of the ferrofluid presence is included in the magnetization $\vec{M}$. In *soft* magnets such as ferrofluids $\vec{M}$ and $\vec{H}$ are aligned. The magnetization curve (i.e. the M *vs.* H curve) and the properties of a typical ferrofluid used in the experiments are shown in **Figure 1** and **Table 1**.

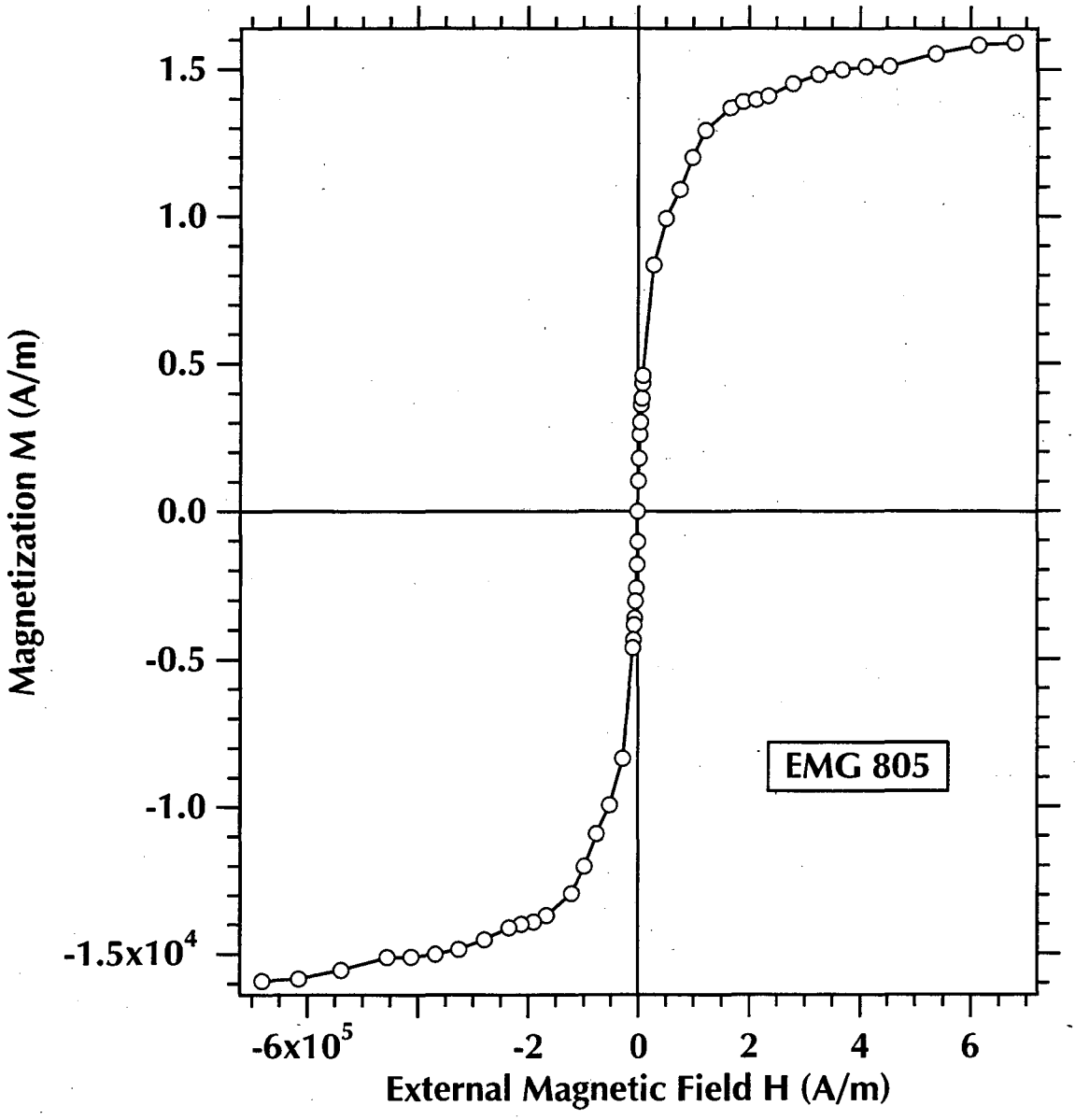

Figure 1. Typical magnetization (M-H) curve for an aqueous-based ferrofluid (EMG 805, Ferrofluidics Corporation, Nashua, NH).

Table 1. Properties of the EMG 805 Ferrofluid	
Viscosity at 27^0	2.5 cp
Magnetite concentration	3.7%
Surfactant concentration	8%
Water concentration	88.3%
Initial magnetic susceptibility	0.49
pH	6.5
Density	1190 kg/m^3
Saturation magnetization	1.6×10^4 A/m

2. Geophysical Studies of FT Performance

2.1. Magnetic Detection of FTs

Tracers are frequently used for characterization of subsurface hydrological properties. Broadly, the method involves the injection of a specific quantity of the tracer fluid through an injection well and monitoring the rate and extent of movement of the fluid by sampling in one or more monitoring wells. One of the drawbacks of this method is that it is invasive in nature, so that the very process of monitoring may disturb the system under study. The use of tracers with magnetic properties can remove this drawback if the injected fluid can be imaged non-invasively by observing the associated magnetic field anomaly at this surface.

The detection of magnetized material in the subsurface is well established in the methodology of applied geophysics [*Telford et al.*, 1990]. One of the earliest magnetic surveys, conducted nearly 100 years ago, was aimed at confirming the outline of the Kiruna iron formation in Sweden. This practice, commonly referred to as the magnetic mapping method, is based on very precise measurements (an accuracy of 20 ppm or ± 1 nT can be achieved routinely) of the earths magnetic field which, on a local scale, is relatively invariant. Thus even very small local variations of the earths field can be associated with the presence of subsurface magnetic material.

The limiting parameter in the detection of the ferrofluid in the subsurface is the susecptibility of the magnetite. The susecptibility is determined both by the magnetic material and by particle size. The susceptibility is a linear function of dilution, and detection depths can be evaluated on a per case basis. In order to assess the feasibility of using dilute ferrofluid as a tracer, we investigate the depth to which a volume containing 1 m^3 of a 15%

solution of EMG 805 water-based ferrofluid (**Table 1**) injected into a medium of $\phi = 0.4$ can be located. For this study we consider 3.3 m^3 of magnetizable material either in the form of a sphere (with a radius $r = 0.92$ m) or in the form of a circular thin plate (with a thickness $d = 0.02$ or $d = 0.10$ m, corresponding to plate radii of $r = 7.75$ m and 6.25 m, respectively). In addition, we discuss the detection of a thin square slab (with $d = 0.02$ m and 0.10 m) and of a vertical semi-infinite cylinder of varying r.

2.2. Theoretical FT Studies

2.2.1. Magnetization

In computing the magnetic anomalies in this study, we assume that the induced magnetization is directly proportional to the inducing field (local ambient magnetic field) and the magnetic susceptibility of the material. We also assume that this quantity is a linear function of the ferrofluid dilution. The magnetite in the EMG 805 ferrofluid has an initial magnetic susceptibility $k_m = 6.16$ MKS units. The concentration of magnetite in the EMG 805 fluid is 3.7%, which would give the ferrofluid a susceptibility of 0.23 MKS. When injected into soil with $\phi = 0.4$, the resulting soil-liquid system has a magnetic susceptibility of 0.091 MKS units at full saturation (i.e., when undiluted). At the postulated 15 % dilution, the corresponding susceptibility $k_m = 0.014$ MKS.

In these calculations we neglect demagnetization. This effect, which is a function of model geometry, tends to weaken the observable effects but is only noticeable in highly magnetized materials. For our spherical model and at the given susceptibility, the demagnetization effect is about 1%. Under these conditions the magnetization of a given object is simply the product of its susceptibility k_m and the intensity of the ambient magnetic field F_0.

2.2.2. Anomalous Magnetic Field for a Sphere

The magnetic field anomaly for a magnetized sphere can be readily computed by considering it to be a magnetic dipole whose moment M is simply the product of the spherical volume V and its magnetization [*Telford et al.*, 1990]. The dipole axis is oriented along the direction of the inducing field. Thus we have,

$$M = V\, k_m\, F_0. \tag{2.1}$$

For the purpose of the model calculations, we consider a simple, high latitude, situation where the sphere is exposed to a vertical inducing field of 47, 000 nT. The field is to be located

using a total field magnetometer, which measures the vertical component of the anomalous magnetic field generated by the presence of the sphere. If the origin of the coordinate system is the center of the sphere (which is located at a depth h below the surface), the observable magnetic anomaly along a traverse over the sphere center is then given by

$$\Delta F = \frac{M}{4\,\pi\,r_d^3}\,\frac{2\,h^2 - x^2}{r_d^2}, \tag{2.2}$$

where

$$r_d^2 = h^2 + x^2. \tag{2.3}$$

Numerical results for traverse profiles over three spheres of different depths but equal magnetic moment are shown in **Figure 2**. From equation (2.1), we note that the magnetic anomaly zero crossings are located at $x = \pm\sqrt{2h}$.

The anomaly maximum lies directly over the center of the sphere ($x = 0$) and has an amplitude of

$$\Delta F_{max} = \frac{M}{2\,\pi\,h^3}. \tag{2.4}$$

For the model under consideration $M = 2.2 \times 10^4$ MKS. Assuming that 1 nT is the smallest detectable ΔF anomaly, then the maximal depth to center at which the 3.3 m^3 sphere can be detected is $h_{max} = 7$ m (**Figure 3**). Note that the maximum depth of detection varies as the $M^{1/3}$ of the sphere. This indicates that doubling the sphere radius doubles the depth of detection at constant saturation and ferrofluid susceptibility. On the other hand, for a constant sphere volume, the fluid susceptibility would have to be raised by a factor of eight (i.e., injection at full strength) in order to achieve a doubling in the depth of detection.

2.2.3. Anomalous Magnetic Field for a Flat Circular Plate

Considering a vertical inducing field and total field measurements, the maximal magnetic anomaly a flat thin circular plate with a radius r occurs over its center and is given by

$$\Delta F_{max} = \frac{M}{2\,\pi\,(z^2 + r^2)^{3/2}}, \tag{2.5}$$

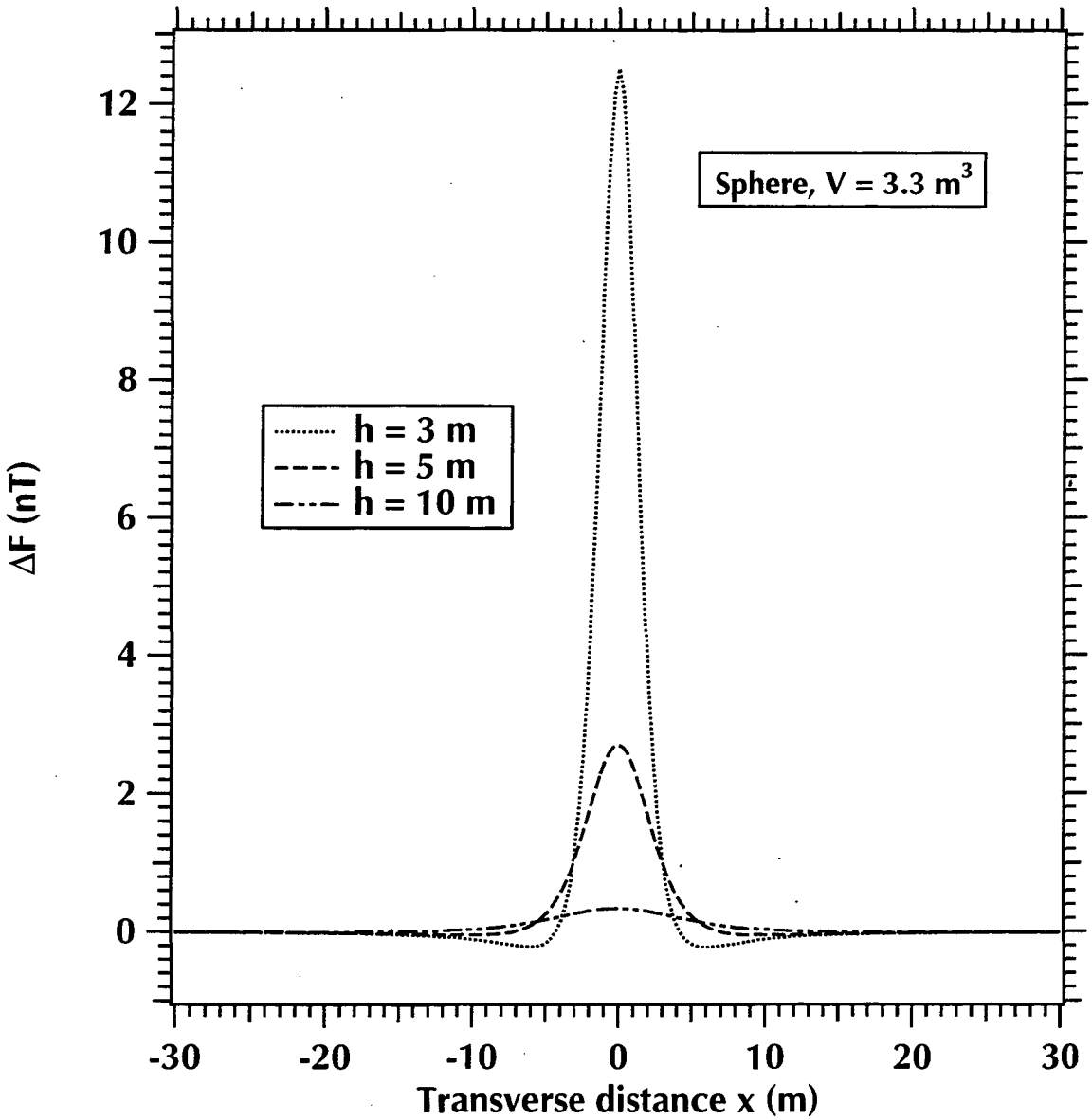

Figure 2. $\Delta F(r, x, h)$ for a $V = 3.3$ m^3 sphere along the x-axis (transverse) at depths $h = 3, 5$ and 10 m.

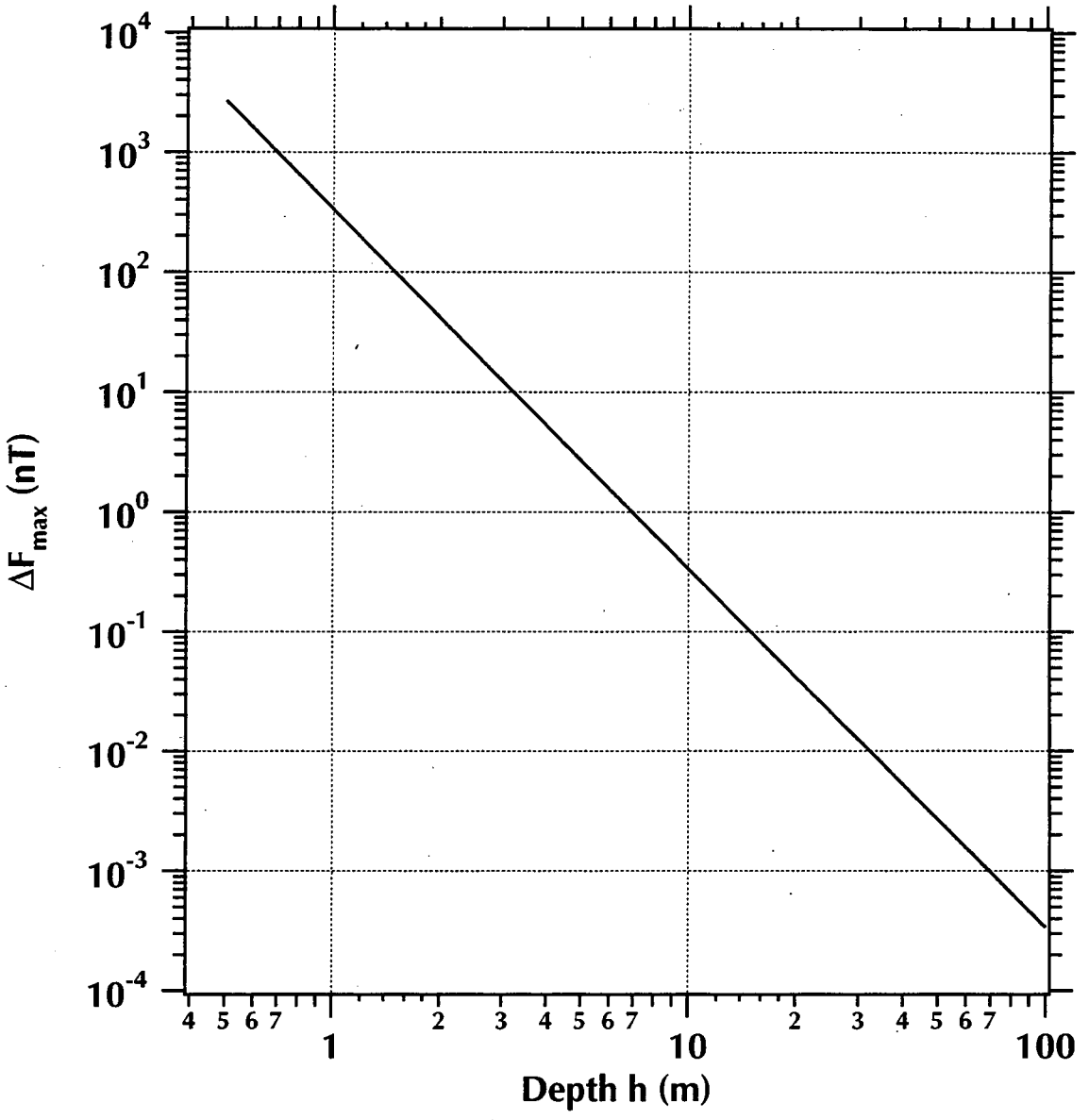

Figure 3. Dependence of $\Delta F_{max} = \Delta F(r, x = 0, h)$ on the depth h to a $V = 3.3$ m^3 spherical anomaly.

where z is the depth to the disk, and M is given by equation (3.1). **Figure 4** shows the ΔF_{max} of a disk with a $V = 3.3$ m^3 and thickness $d = 0.1$ m and 0.02 m. At $z > r$, the anomaly due to the plate approaches that of a dipole.

If we take the disc and sphere volume to be equal, we can determine a relationship between h_{max} (see section 2.2.1) and the maximal depth of detection for the disc, z_{max}. The two are related as

$$h_{max} = \sqrt{z_{max}^2 + r^2} \qquad \text{and} \qquad z_{max} = \sqrt{h_{max}^2 - r^2}, \tag{2.6}$$

indicating that for an equal volume of material $z_{max} > h_{max}$. In the present case (in which $V = 3.3$ m^3), the $d = 0.02$ m plate ($r = 7.25$ m) can be detected to a depth of $z_{max} = 7$ m, i.e., at nearly the same depth as the sphere but 0.9 m lower than the sphere top. When $d = 0.1$ m, the disk r decreases to 3.25 m, the magnetic anomaly over its center increases and z_{max} increases to about 10 m. As before, demagnetization is neglected in these calculations. Note that when $r > z$, the magnetic field anomaly generated by the disk at its edges may exceed that observed over its center.

2.2.4. Anomalous Magnetic Field for a Flat Rectangular Plate

For a flat square plate at depth h, with width $2a$, length $2b$ and thickness d, the magnetic anomaly is given by the equation [*Bhattacharyya*, 1964]

$$\Delta F = \frac{k_m F_0 d}{4\pi}\left[\frac{2ba_2}{(a_2^2+h^2)\sqrt{a_2^2+b^2+h^2}}\left(1+\frac{h^2+a_2^2}{h^2+b^2}\right) - \frac{2ba_1}{(a_1^2+h^2)\sqrt{a_1^2+b^2+h^2}}\left(1+\frac{h^2+a_1^2}{h^2+b^2}\right)\right], \tag{2.7}$$

where

$$a_1 = x - a \qquad \text{and} \qquad a_2 = x + a, \tag{2.8}$$

and x is the detector position on the surface with respect to the center of the plate. The transverse profiles of rectangular plate with a $V = 3.3$ m^3, $d = 0.02$ m and 0.10 m at $h = 0.5$, 1,5, and 10 m are given in **Figure 5**. As with the thin disk, when $h << 2a$, the edges of the plate display a higher anomalous reading that the center. The maximum anomaly does not occur at the center of the plate (i.e., at $x = y = 0$) but near the edge of the plate.

The anomaly ΔF at the center ($x = 0$) of a square plate ($a = b$) is given by the equation

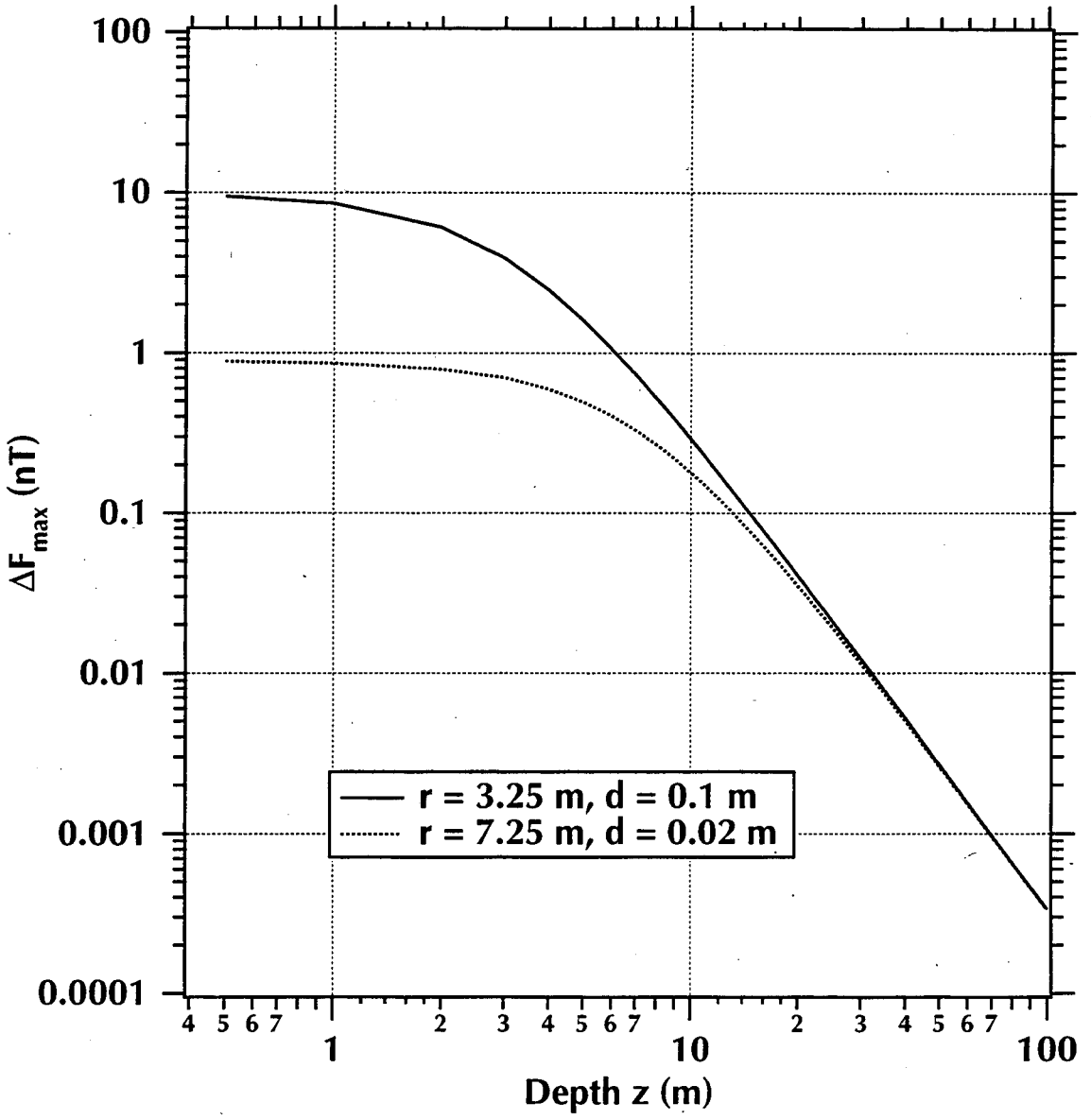

Figure 4. Dependence of $\Delta F(r, d, x = 0, h)$ on the depth h to a $V = 3.3$ m^3 disk-shaped anomaly of thickness d and radius r.

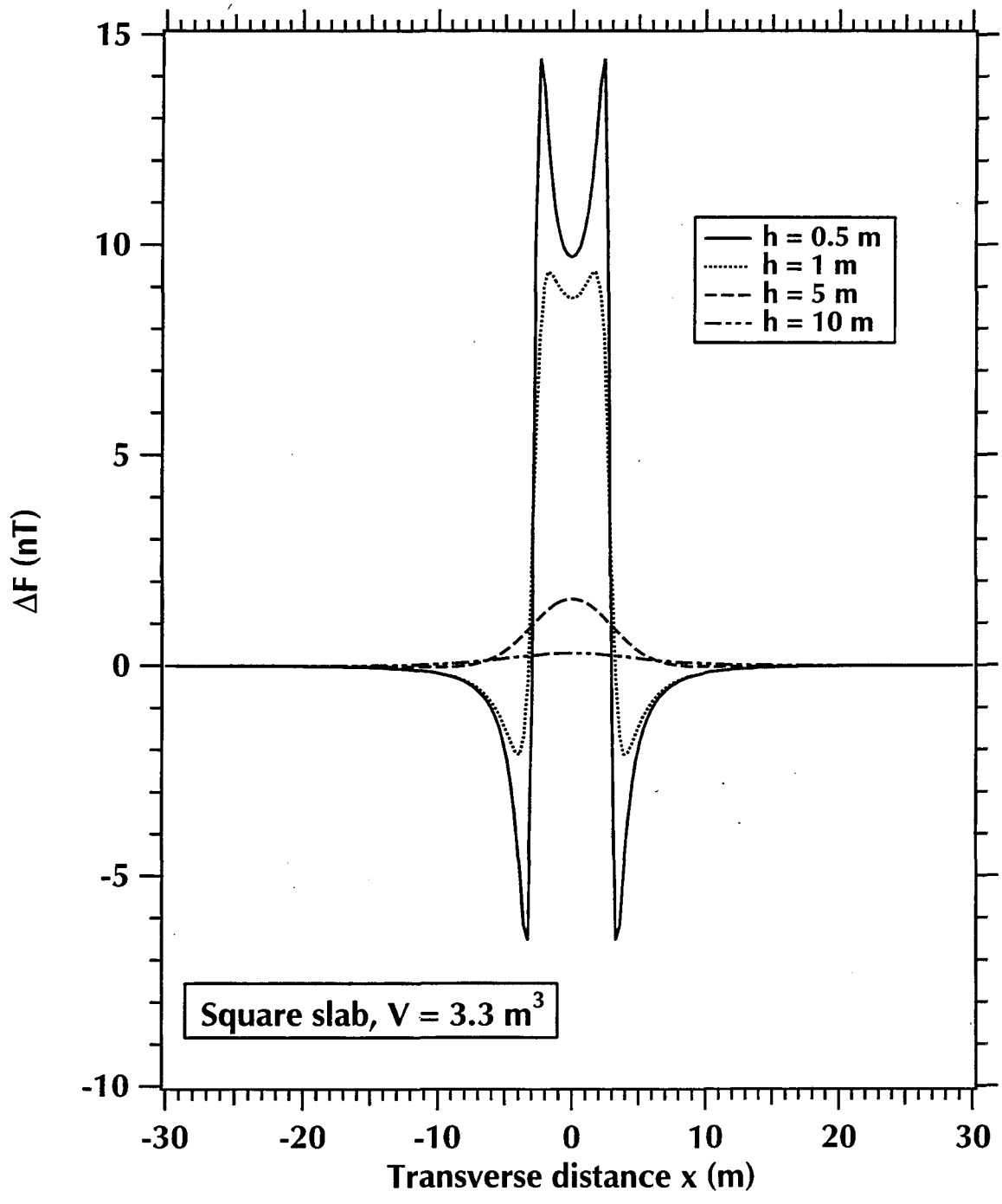

Figure 5. $\Delta F(a, d, x, h)$ for a $V = 3.3$ m^3 square slab anomaly (of width a and thickness d) along the x-axis (transverse) at various depths h.

$$\Delta F = \frac{k_m F_0 d}{\pi} \left[\frac{a^2}{(a^2+h^2)\sqrt{2a^2+h^2}} \right]. \qquad (2.9)$$

The $\Delta F(x=0,h)$ for a aquare slab of thickness $d = 0.02$ and 0.10 m are shown in **Figure 6**. The results are similar to those of the disk, with the anomaly approaching that of a dipole as h increases.

2.2.5. Anomalous Magnetic Field for an Infinite Vertical Cylinder

A vertical cylinder at a depth to its top z much less than its length can be approximated by a monopole, in which case the anomaly is given by [*Breiner*, 1973]

$$\Delta F = \frac{k_m F_0 r^2}{4 r_d^2}, \qquad r_d^2 = x^2 + z^2 \qquad (2.10)$$

where r is the cylinder radius and x is the distance from the projection of the cylinder center to the surface. The transverse profiles over a vertical cylinder of $r = 0.5$ m, and $z = 3$ and 5 m are given in **Figure 7**. The detection depth of the cylinder is on the same order of the sphere discussed in Section 6.2.2. The anomaly over the center of the cylinders of $r = 0.3$ and 0.5 m are shown in **Figure 8**. The maximum depth of detection for these cylinders are 4 and 6 meters, respectively.

2.3. Experimental FT Investigations

The feasibility of using of ferrofluids as tracers was investigated in laboratory magnetometer surveys of various FT shapes which involved comparisons between the measured and the theoretically predicted values. A three axis miniature fluxgate magnetometer (model APS534, Applied Physics Systems, Mountain View, CA) was used in these experiments.

To effectively calculate the expected anomaly and to interpret the measured anomaly, the magnetic baseline was first determined by measuring the ambient field. These measurements had to be made away from buildings and mechanical structures in order to alleviate magnetic interferences and allow a clear and consistent signal. Therefore, all measurements were conducted outdoors away from buildings, power lines and/or other large metallic structures, with the magnetometer placed on a carefully leveled plywood board resting on a resin table.

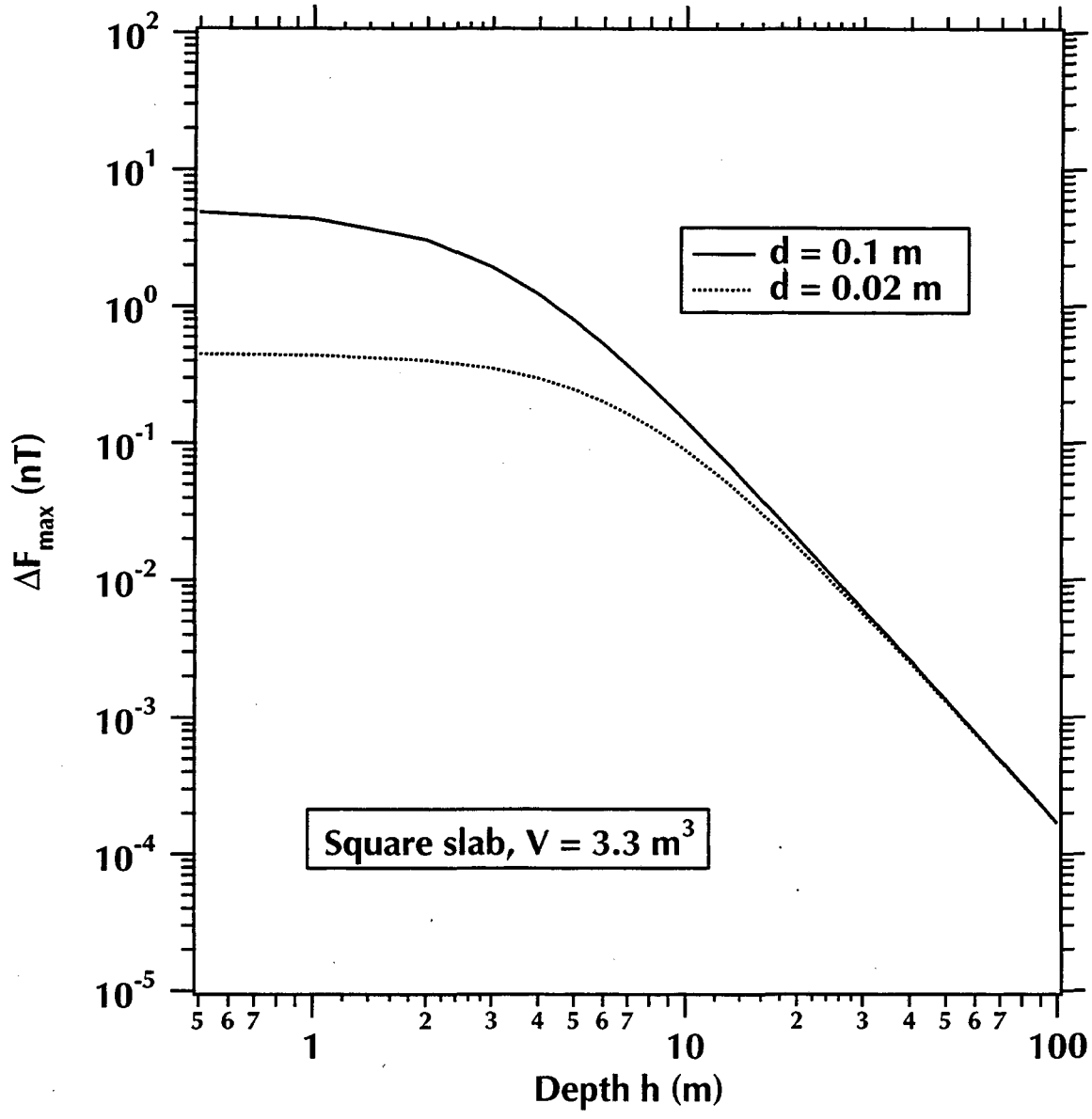

Figure 6. Dependence of $\Delta F(a, d, x = 0, h)$ on the depth h to a square slab anomaly of width a, thickness d and constant volume $V = 3.3$ m^3.

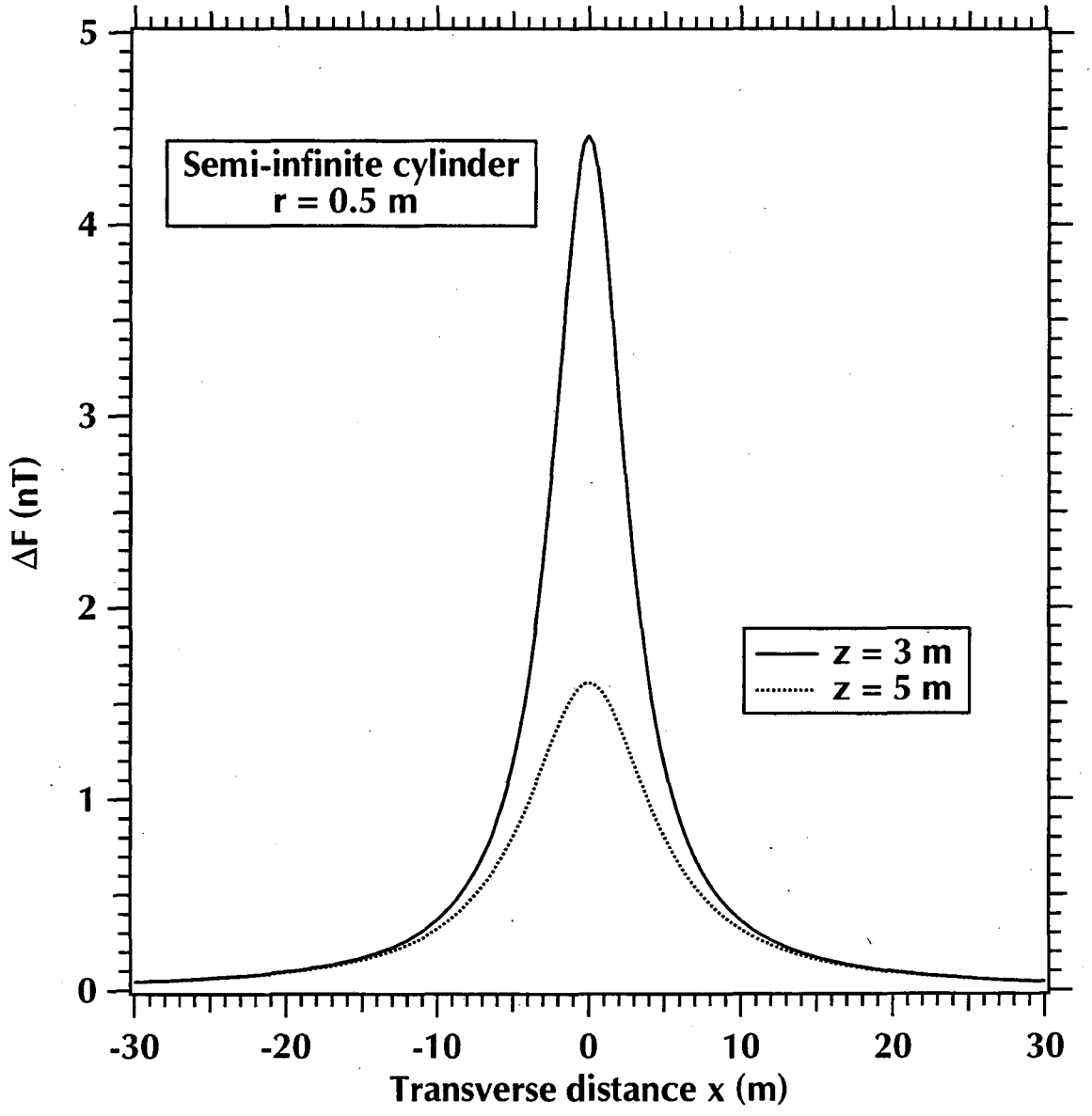

Figure 7. $\Delta F(r, x, z)$ for a semi-infinite cylinder of radius $r = 0.5$ m.

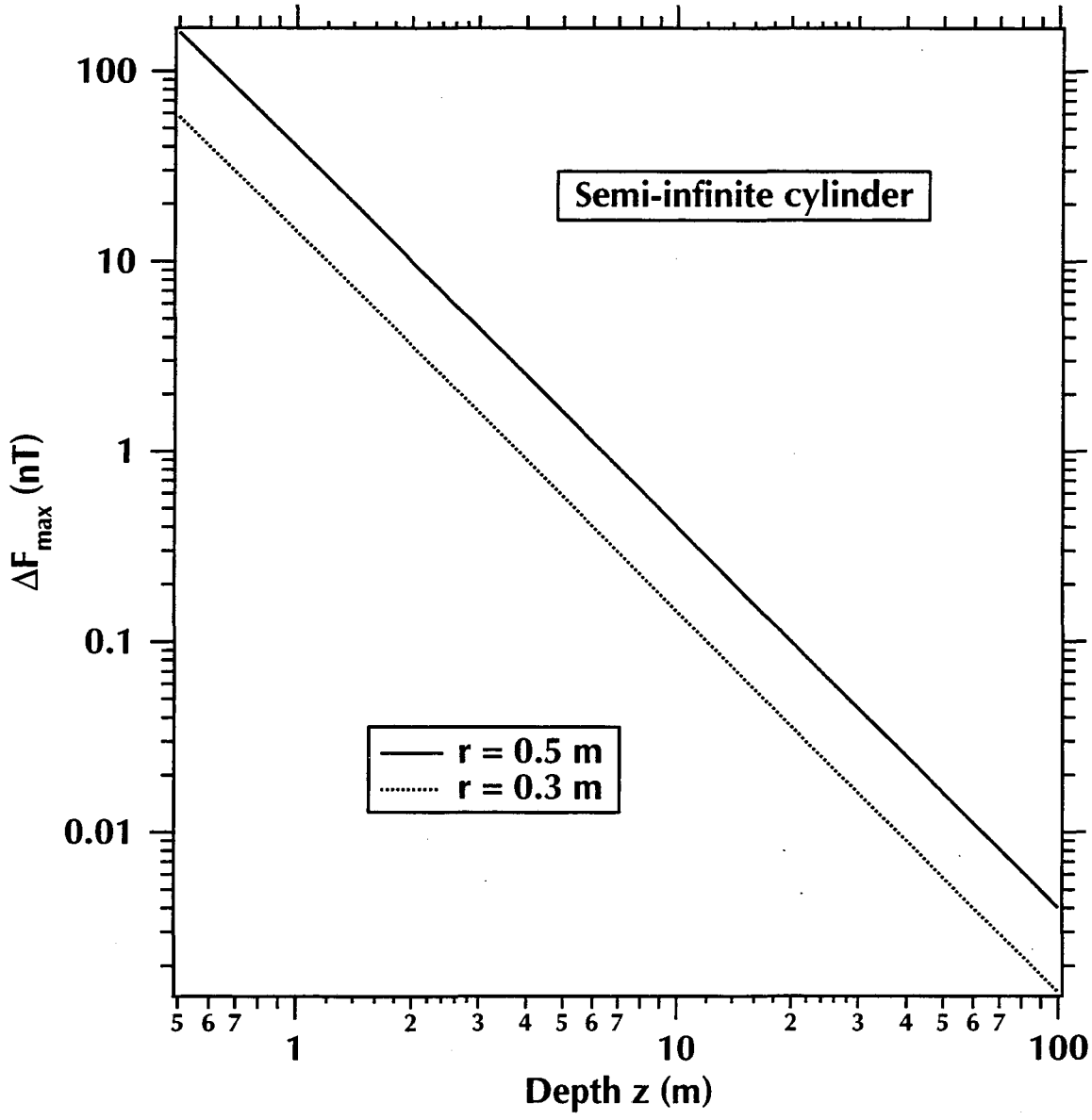

Figure 8. Dependence of $\Delta F_{max} = \Delta F(r, x = 0, z)$ on the depth z to a semi-infinite cylindrical anomaly of radius r.

The ambient field is a vector quantity and therefore has components in the x, y, and z direction. For the present experiments, the vertical component of the field was maximized and the resulting vertical anomaly was recorded. A set of typical ambient field measurements are given in **Table 2.**

The magnetometer had a excitation voltage of ± 10 V and an output voltage of ± 5 V. The output voltage for the H_x, H_y and H_z components of the ambient magnetic field was measured by a digital multimeter and was manually logged. To minimize noise, the magnetometer was fixed in position and the anomaly-inducing FT volume was moved in relation to the probe over the gridded surface of the board (0.01×0.01 m grid size). After first ensuring that the inducing ambient field was consistent over the surface of the board, the magnetometer was aligned with the magnetic north. This maximized the resultant signal in the EW and vertical directions.

A major consideration in achieving reliable anomaly measurements is to minimize the noise in ambient fields. Such noise increases due to solar effects and anthroprogenic activities during the daylight hours. Periodic magnetic storms can also increase the noise level by an order of magnitude. Therefore, care has to be taken in the selection of the location and time of the magnetic measurements.

In the following experiments, the magnetometer was placed on the level, gridded board, with the main axis of the magnetometer pointed toward the magnetic north. To measure the anomaly from the ferrofluid samples (prepared as described in the following section), the samples were moved along a line perpindicular to the axis of the magnetometer (**Figure 9**). With this configuration, the vertical anomaly at the magnetometer position is negative. Although field measurements routinely achieve detection limits on the order of 1 nT, in these laboratory experiments the detection limit was about 2 nT.

Table 2. Typical Ambient Field Measurements

Component	Field (nT)
H_z (vertical)	42,000
H_x (EW)	22,000
H_y (NS)	750
Resultant (declination 18°)	47,000

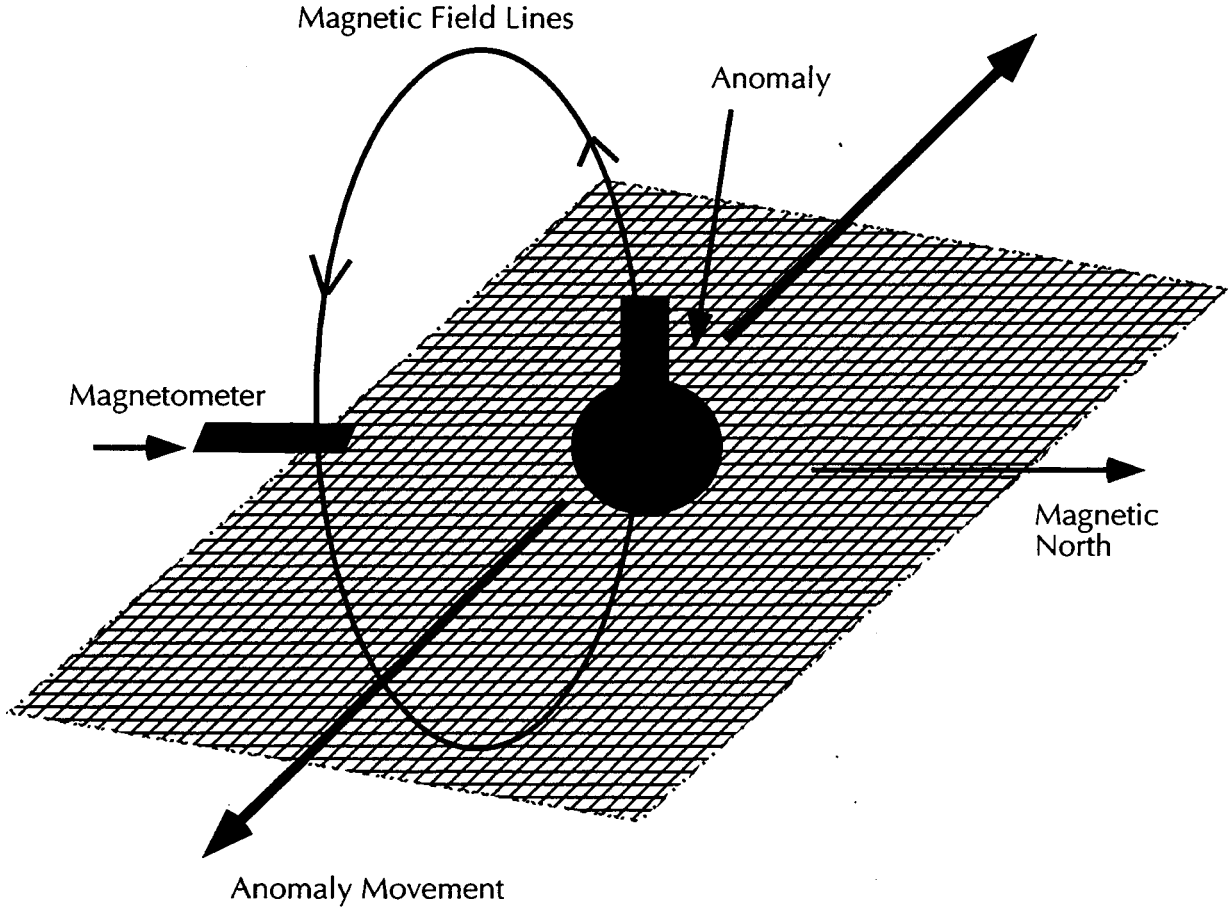

Figure 9. A schematic of the experimental approach in the measurement of the FT-induced anomalies.

2.3.1. *Spherical Anomaly*

To model the spherical anomaly described above, a 100 ml spherical flask was filled with 100% (i.e., undiluted) EMG 805 ferrofluid. The resulting anomaly had a $V = 105$ ml. Using equation (6.4) and the $V = 3.3$ m^3 sphere as a reference, a general scaling relationship can be obtained to predict the anomaly. Assuming that the inducing fields are the same, we derive

$$\frac{h_1}{h_2} = \left(\frac{k_{m1}\, V_1}{k_{m2}\, V_2}\right)^{1/3}. \tag{2.11}$$

If h_1 is the depth to the $V_1 = 105$ ml flask and h_2 is the depth to the $V_2 = 3.3$ m^3 sphere, $k_{m1} = 0.23$ MKS is the susceptibility of the undiluted EMG 805 ferrofluid in the flask and $k_{m2} = 0.014$ MKS is the susceptibility of 15% ferrofluid solution in the V_2 sphere, then

$$\frac{h_1}{h_2} = 0.08,$$

from which the maximum detection depth for the V_1 anomaly is determined as $h_{max} = 0.56$ m.

Predictions and measurements of the spherical anomaly-induced ΔF along the x-axis (transverse) at $h = 0.055$, 0.08, and 0.12 m are shown in **Figures 10** through **12.** As the distance from the magnetometer increases, the maximum anomaly decreases and broadens. Under the conditions of the experiments, the ΔF at $h = 0.12$ m is only four times the detection limit, and therefore considerable noise is apparent in the data. For all three tranverses, however, a good match between predictions and measurements (in terms of anomaly shape, height and width) is observed.

The flask of ferrofluid was moved along the center line (i.e. along h at $x = 0$) from $h = 0.035$ m to $h = 0.28$ m, and the maximum anomaly peak ΔF_{max} was recorded as it decreased with h. **Figure 13** shows a good agreement between the measured and the predicted ΔF_{max}. The scattering at the larger h values is due to the proximity of the measured anomaly to the limit of detection of the instrument.

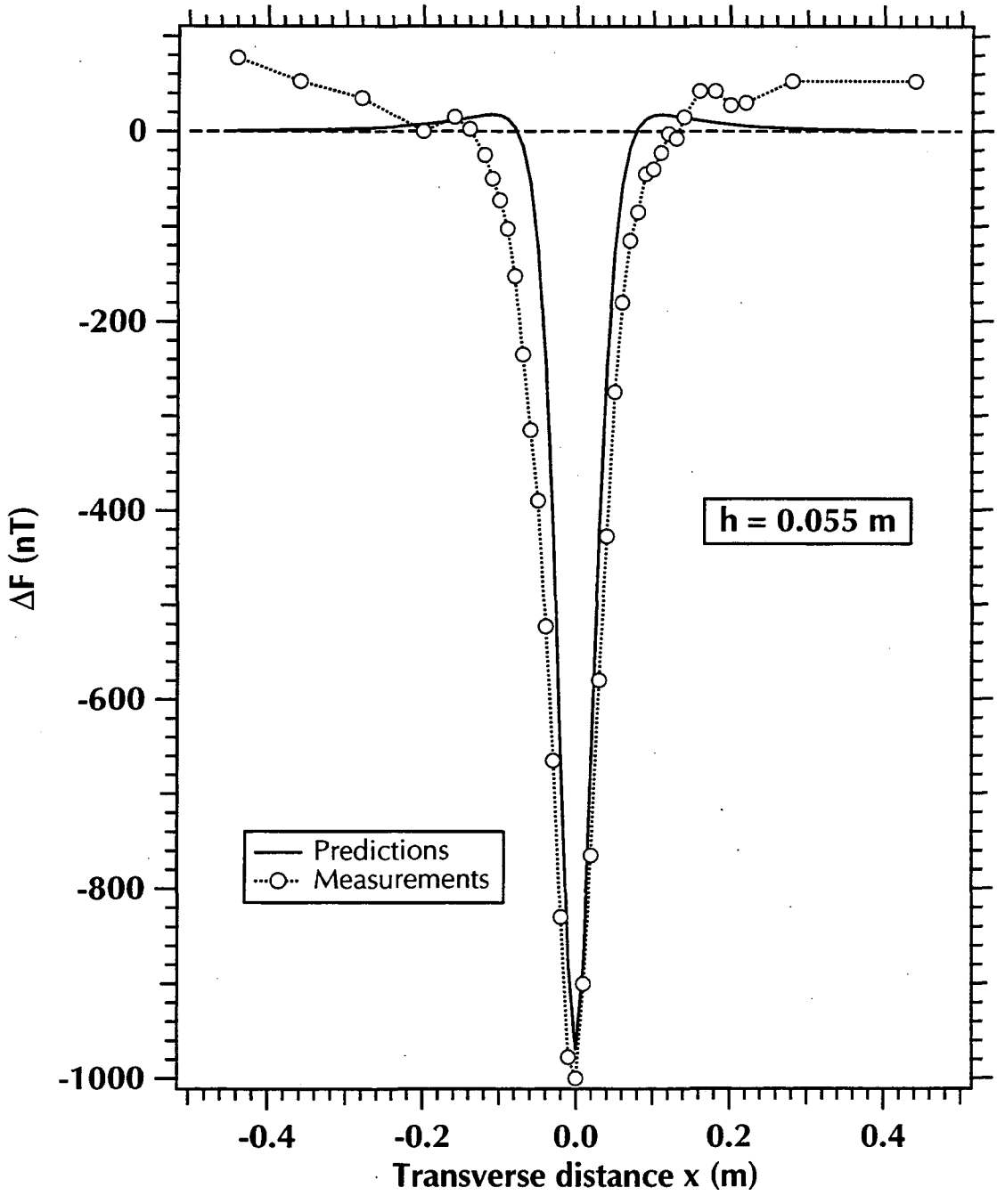

Figure 10. Calculated and measured ΔF for a sphere with $V = 100$ ml at a depth $h = 0.055$ m.

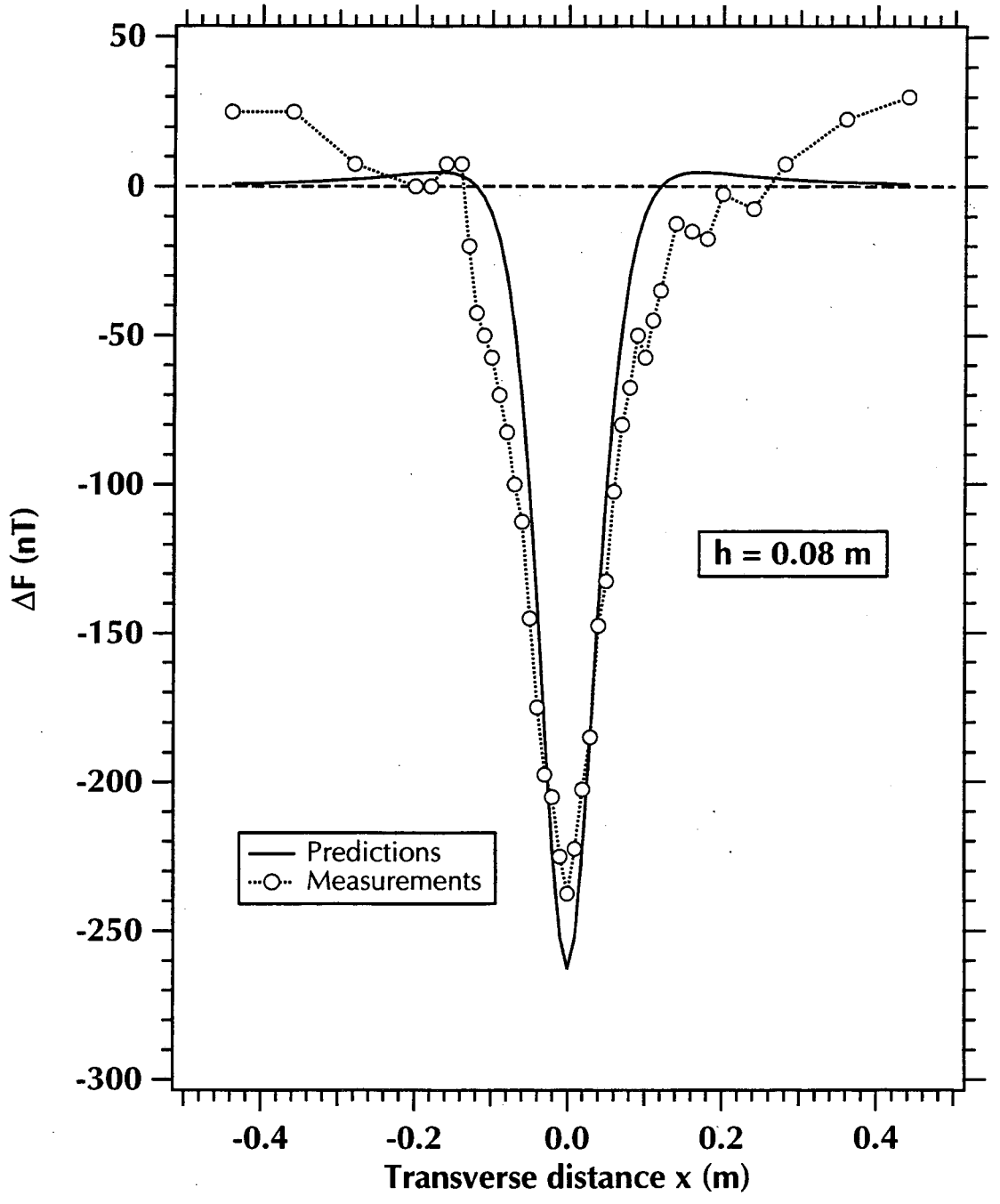

Figure 11. Calculated and measured ΔF for a sphere with $V = 100$ ml at a depth $h = 0.085$ m.

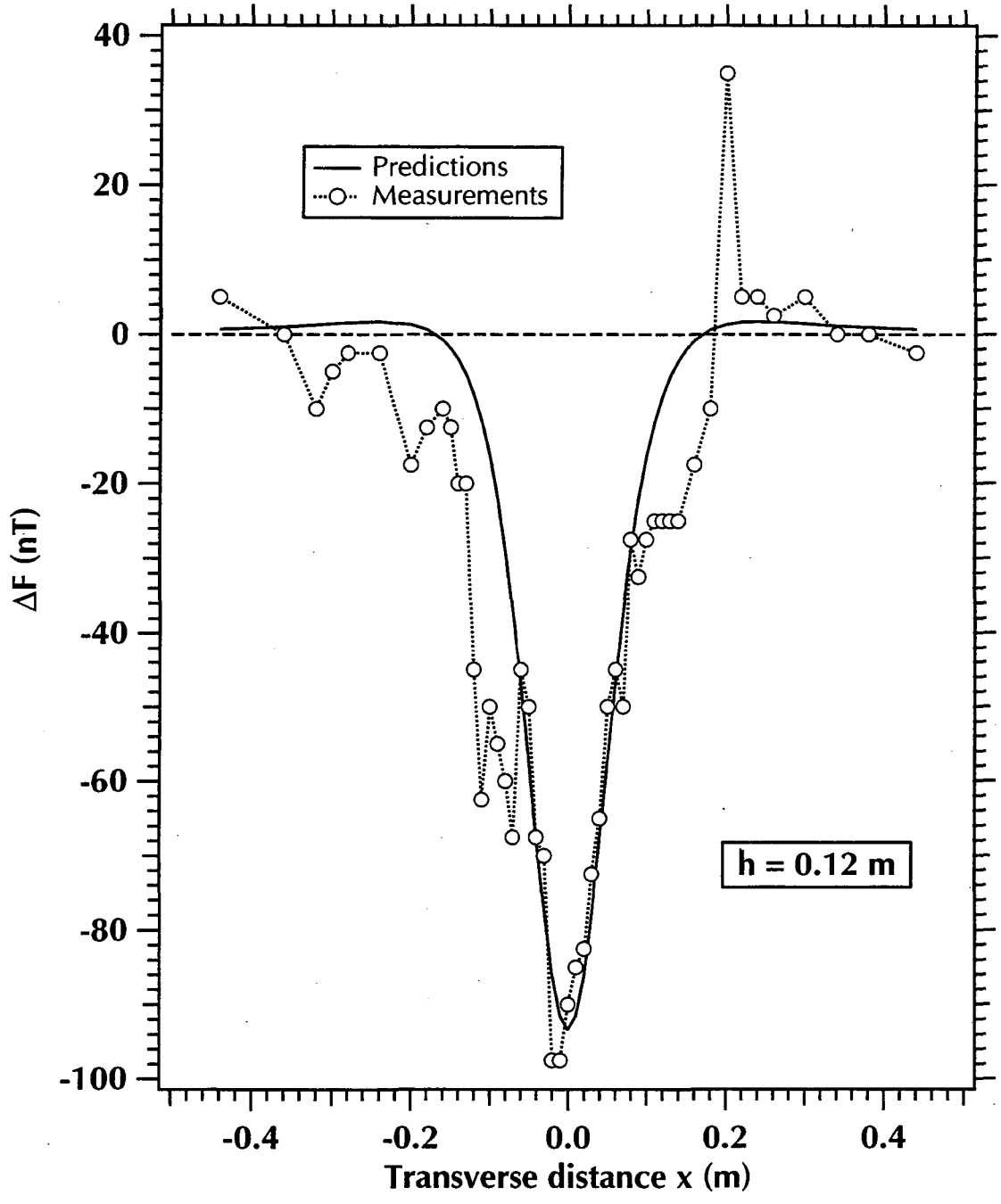

Figure 12. Calculated and measured ΔF for a sphere with $V = 100$ ml at a depth $h = 0.12$ m.

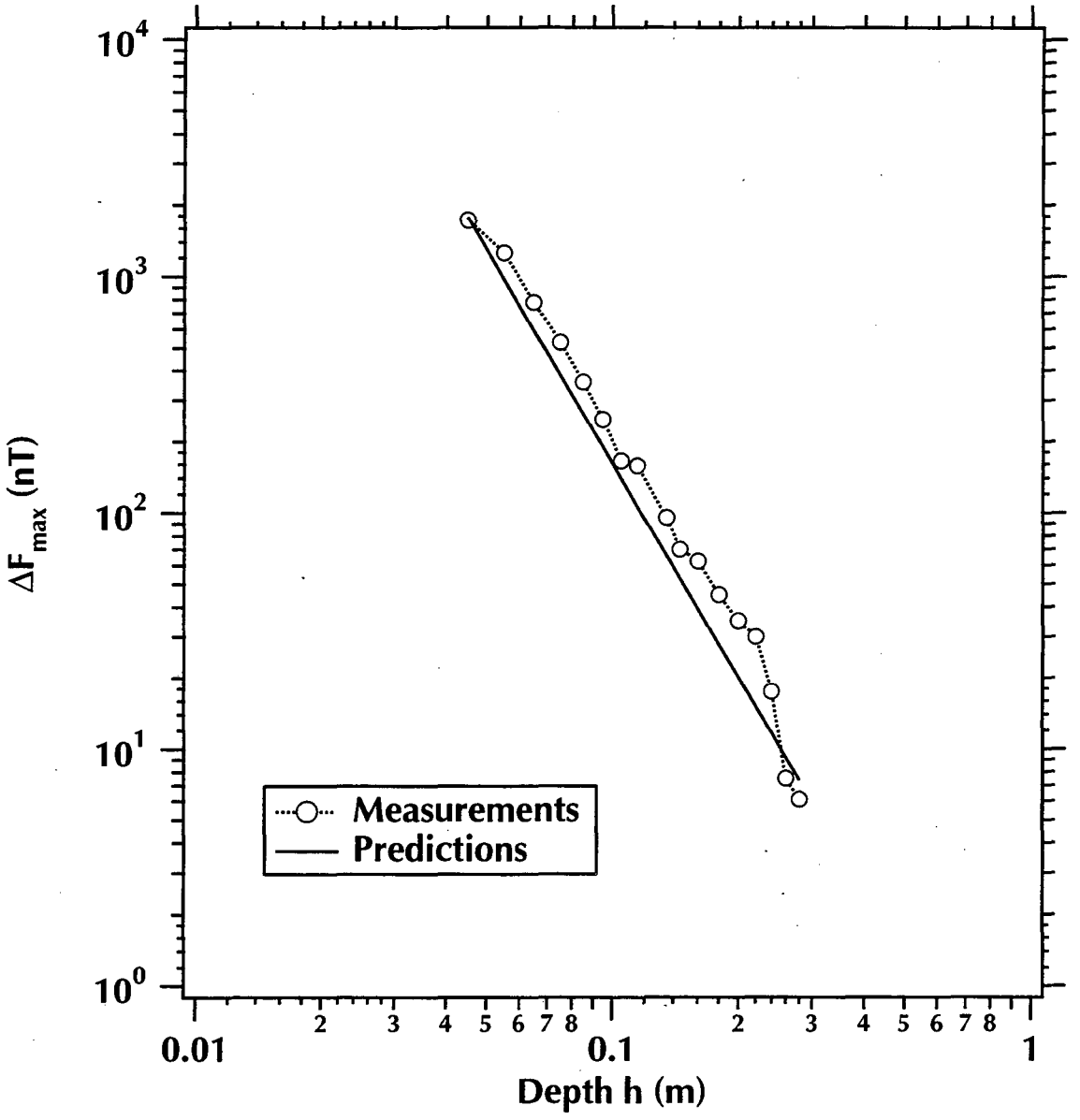

Figure 13. Calculated and measured $\Delta F_{max} = \Delta F(x = 0, h)$ for a buried sphere with a $V = 100$ ml.

2.3.2. Cylindrical Anomaly

An anomaly was created with a $V = 100$ ml cylinder ($r = 0.02$ m) filled with EMG 901 ferrofluid (**Table 3**). Measurements of the cylinder-induced anomaly along the transverse axes at $z = 0.03$, 0.05, and 0.09 m are shown in **Figure 14** through **16**, and are in very good agreement with the predictions of equation (2.10). The cylinder-induced anomaly is broader than that for the sphere, and does not have an x region in which $\Delta F < 0$.

Figure 17 shows a comparison of measured and predicted $\Delta F_{max} = \Delta F(x = 0, z)$ for 0.03 m $\geq z \geq$ 0.28 m. A very good agreement between the two data sets is observed.

2.3.3. Rectangular Slab Anomaly

A flat plate anomaly was created using a rectangular container with dimensions $0.03 \times 0.08 \times 0.12$ m. The container was filled with Monterey sand, and was then saturated with a 30% solution of EMG 805 ferrofluid. The susceptibility of this rectangular slab system k_{ms} is computed as $k_m = 0.0306$ MKS.

The flat plate anomaly was positioned so that the distance between its long edge and the magnetometer (i.e., the depth h) was 0.03 m. A comparison of the ΔF measurements to predictions is shown in **Figure 18**. Although a scattering of the measurements is observed in the vicinity of the anomaly edges, there is a good agreement between measurements and predictions in terms of ΔF shape, width and magnitude.

Table 3. Properties of the EMG 901 Ferrofluid	
Viscosity at 27^0	11 cp
Magnetite concentration	9.89%
Surfactant concentration	15%
Light mineral oil concentration	75.11%
Initial magnetic susceptibility	0.337 MKS
Density	1360 kg/m^3
Saturation magnetization	3.1×10^4 a/m

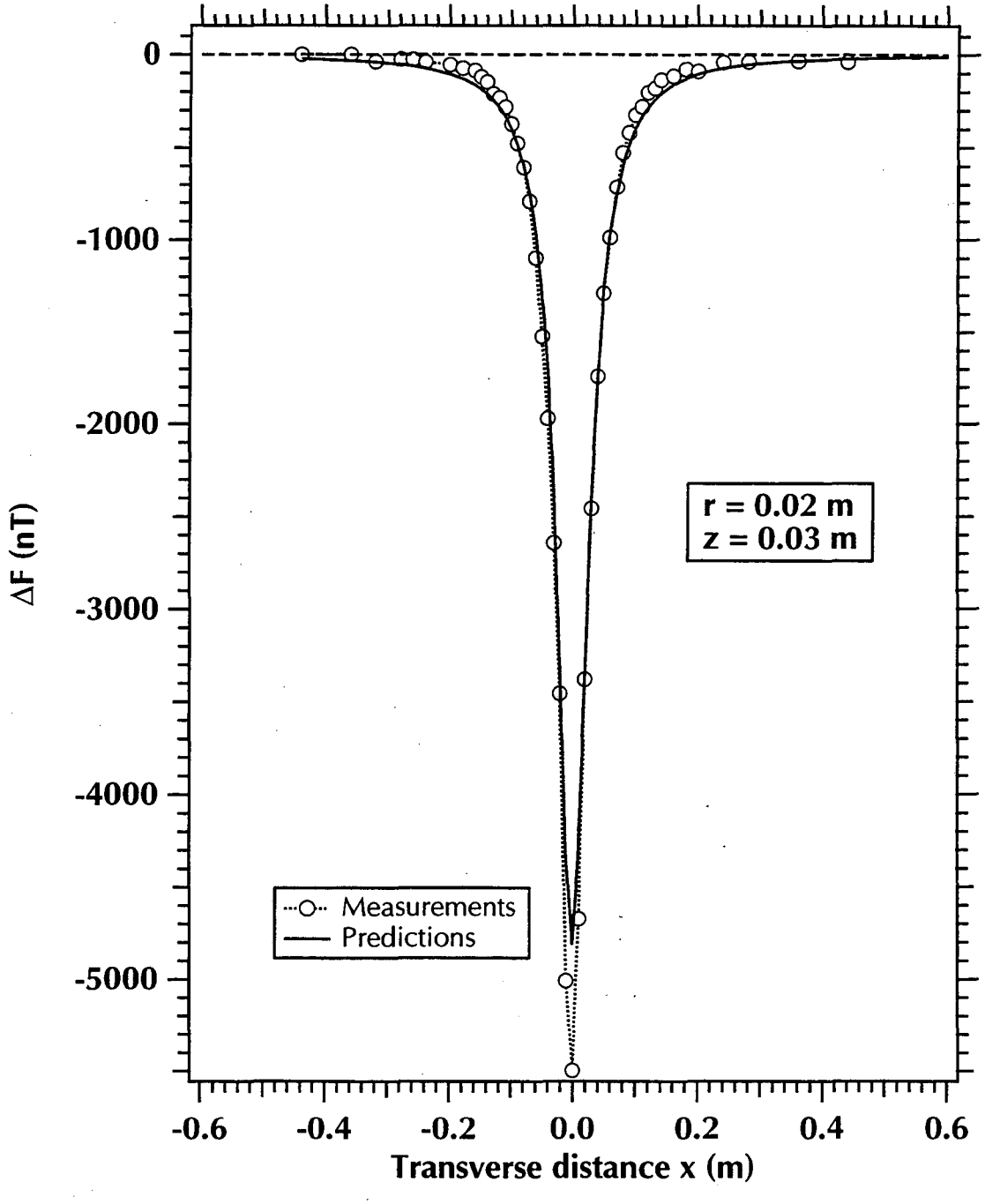

Figure 14. Calculated and measured ΔF for a semi-infinite cylinder with $r = 0.02$ m at a depth $z = 0.03$ m.

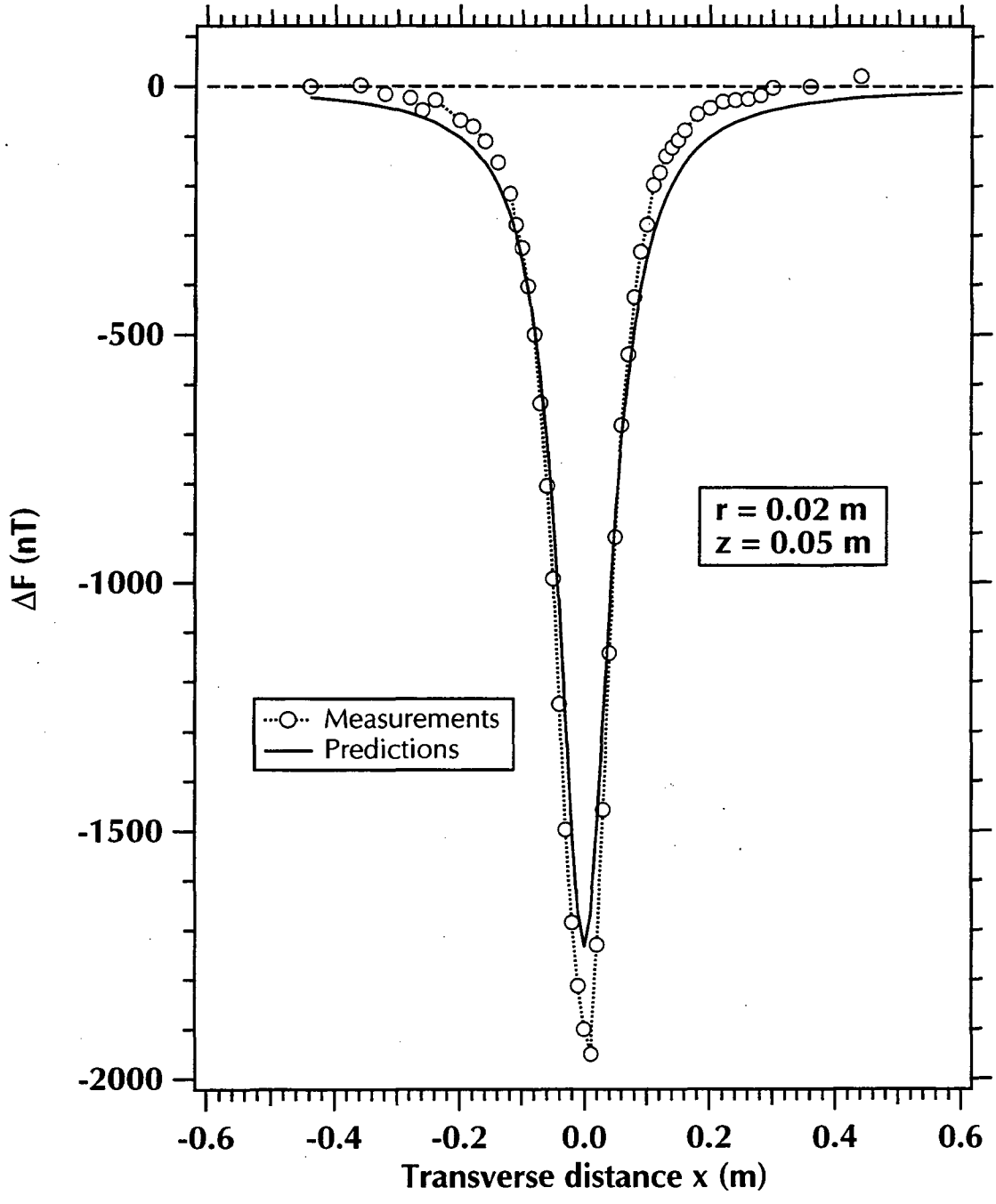

Figure 15. Calculated and measured ΔF for a semi-infinite cylinder with $r = 0.02$ m at a depth $z = 0.05$ m.

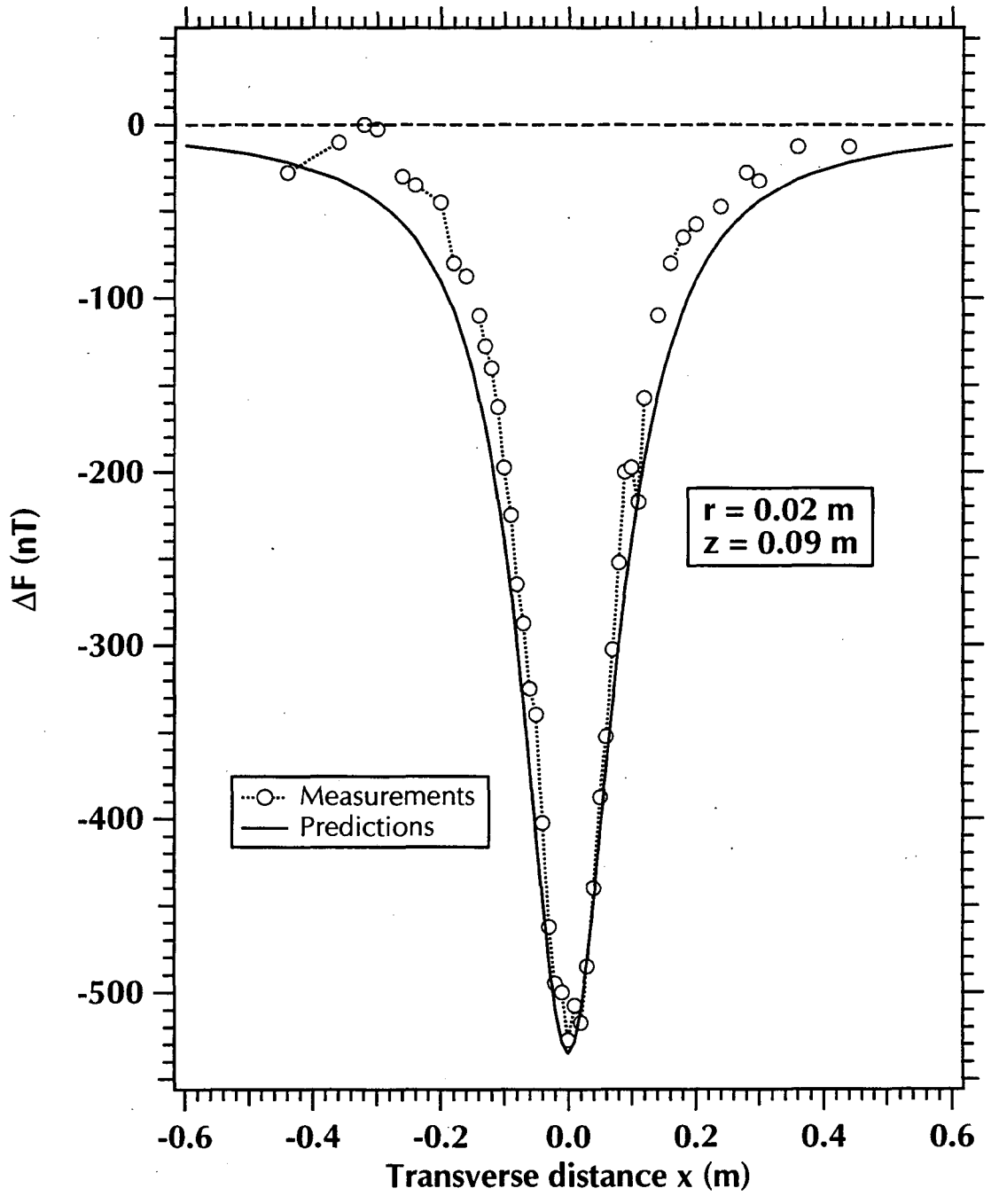

Figure 16. Calculated and measured ΔF for a semi-infinite cylinder with $r = 0.02$ m at a depth $z = 0.09$ m.

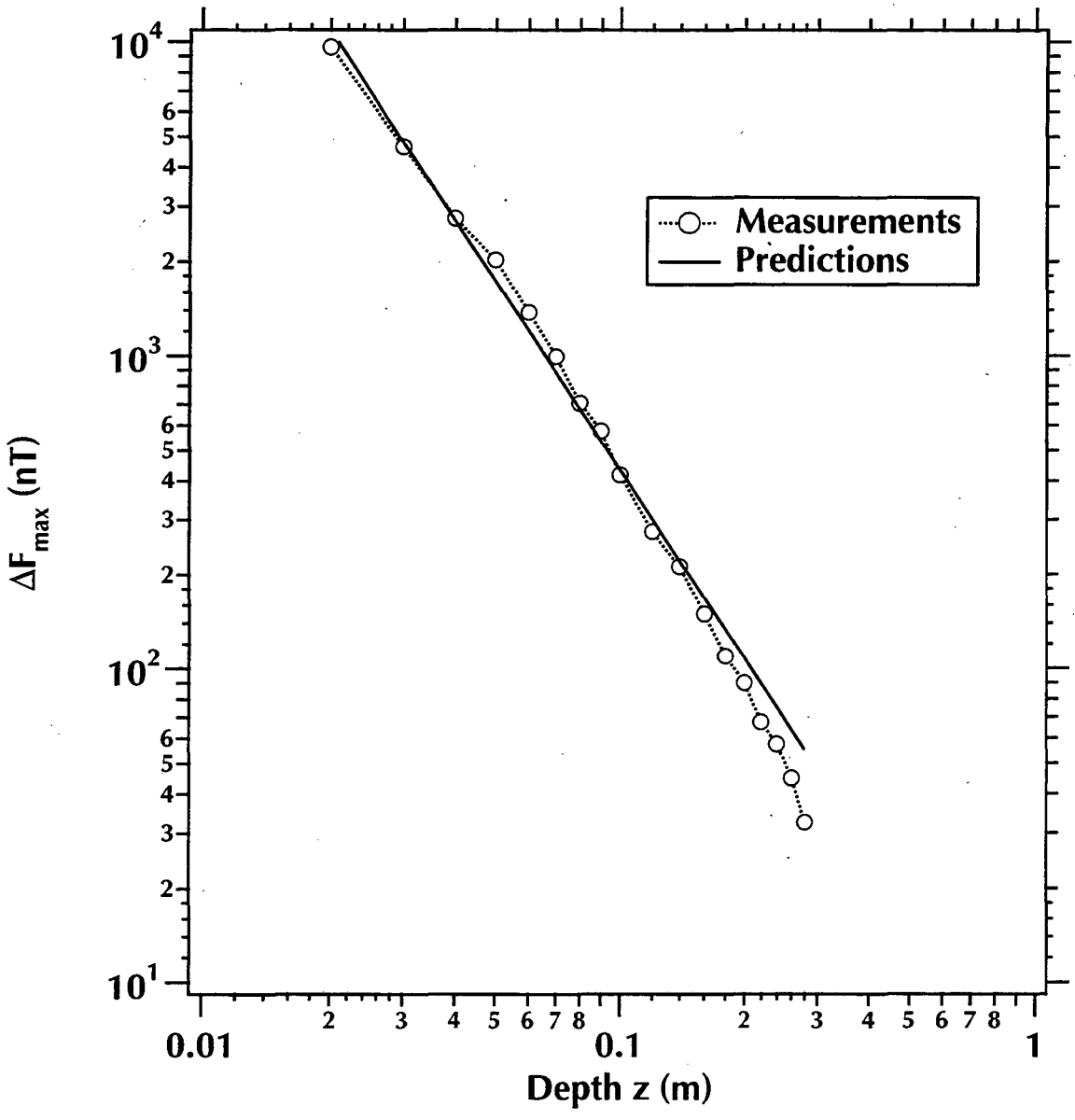

Figure 17. Calculated and measured $\Delta F_{max} = \Delta F(x = 0, z)$ for a semi-infinite cylinder with $r = 0.02$ m.

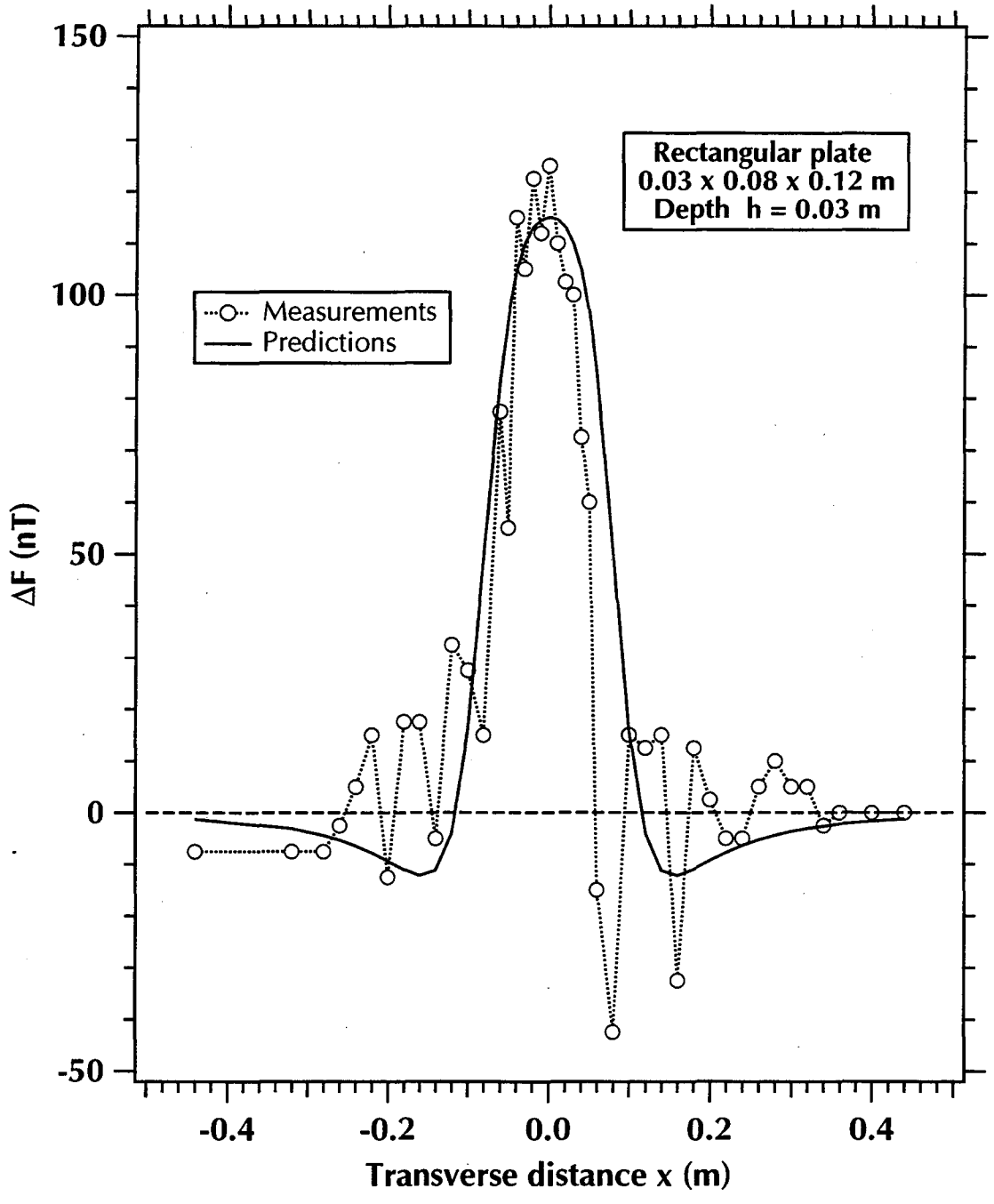

Figure 18. Calculated and measured ΔF for a $0.03 \times 0.08 \times 0.12$ m rectangular plate at a depth $h = 0.03$ m.

2.4. Discussion

Care must be exercized in the application of FT-based tracer techniques to minimize the magnetic noise, which can obscure small anomaly signals and significantly increase detection limits. One limiting factor in anomaly detection is the low susceptibility of the ferrofluid, which is a function both of the particle size and the material properties of the magnetite in the ferrofluid. Larger magnetite particles increase the FT susceptibility, and thus the detection depth. The particle size of the magnetite is determined by the manufacturing process. The stability of the fluid is dependent on a force balance between particle interaction and repulsion between the surfactants attached to the fluid particles. Although the particle size can be increased, this affects adversely the FT stability [*Rosensweig*, 1985]. In addition, a FT with a larger particle size may exhibit increased (and undesirable) filtration effects when injected into a porous medium. New FTs, with the same particle size but with higher susceptibility (such as NdFeB-based FTs), could increase the detection depths of FTs and improve their tracer potential.

3. SUMMARY AND CONCLUSIONS

Ferrofluids are stable colloidal suspensions of magnetic particles in various carrier liquids [*Raj and Moskowitz*, 1990] with high saturation magnetizations. The solid, magnetic, single-domain particles have an average diameter of $3 - 15$ nm, and are covered with a molecular layer of a dispersant. Thermal agitation (Brownian motion) keeps the particles suspended, while the dispersant coating prevents the particles from agglomeration. Ferrofluids are superparamagnetic and move as a homogeneous single-phase fluid under the influence of a magnetic field, with no separate consideration for the magnetic particles and the carrier liquid. This attribute is responsible for the unique property of ferrofluids that they can be manipulated in virtually any fashion, defying gravitational or viscous forces in response to external magnetic fields [*Chorney and Mraz*, 1992].

In this report we review the results of our investigation of the potential of ferrofluids to trace the movement and position of liquids injected in the subsurface using geophysical methods. To investigate the feasibility of using ferrofluids as tracers (FT) in the subsurface, theoretical and experimental investigations of the magnetic anomalies they induce were conducted. The results of these studies confirm that the anomaly behavior can be accurately predicted by existing mathematical models.

Ferrofluid for **T**racing liquids (FTs) cast a strong electro-magnetic signature, and are used commercially for magnetic pattern recognition in magnetic tapes, hard and floppy disks, and crystalline and amorphous alloys. The high saturation magnetization in the FTs provides a signature sufficiently strong for magnetic detection methods at low loading volumes (i.e. $1 - 5\%$). We investigated exploiting this property to develop a method for monitoring of liquid movement and position during injection using electromagnetic methods. FTs can also

provide a significant detection and verification tool in containment technologies, where they can be injected with the barrier liquids to provide a strong signature allowing determination of the barrier geometry, continuity and integrity. FTs can also be used to identify high-permeability pathways, and thus allow the design of more effective remediation systems.

We demonstrated the feasibility of using conventional magnetometry for detecting subsurface zones of injected FTs used to trace liquids injected for remediation or barrier formation [*Borglin et al.*, 1998]. The geometrical shapes considered were a sphere, a thin disk, a rectangular horizontal slab, and a cylinder. Simple calculations based on the principles of magnetometry were made to determine the detection depths of FTs. Experiments involving spherical, cylindrical and horizontal slabs showed a very good agreement between predictions and measurements.

4. REFERENCES

Bhattacharyya, B.K., Magnetic Anomalies due to prism-shaped bodies with arbitrary polarization, Geophysics, XXIX(4), 517-526, 1964.

Bailey, R.L., Lesser known applications of ferrofluids, J. Magnetism Magnetic Mater., 39(1,2), 178-182, 1983.

Becker, A., and L.S. Collett, Magnetic losses in lunar materials, Earth and Planetary Science Letters, 41, 139-142, 1978.

Borglin, S., and G.J. Moridis, Experimental investigations of magnetically-driven flow of ferrofluids through porous media, LBL Report No. 40126, Lawrence Berkeley National Laboratory, March 1998.

Borglin, S., A. Becker, and G.J. Moridis, Magnetic detection of ferrofluid injection zones, LBL Report No. 40127, Lawrence Berkeley National Laboratory, Berkeley, California, March 1998.

Breiner, S., Applications Manual for Portable Magnetometers, Geometrics, Sunnyvale, CA, 1973.

Chorney, A.F., and W. Mraz, Hermetic sealing with magnetic fluids, Machine Design, 79-82, May 1992.

Ferrofluidics, Application Note: Ferrofluids in the biomedical field, Ferrofluidics Corp., 1992.

Hood, P., and D.J. McLure, Gradient measurements in ground magnetic prospecting, Geophysics, 30, 403-410, 1965.

Hsu, S.K., S.-J. Sibuet, and C.-T. Shyu, High resolution detection of geologic boundaries from potential field anomalies, Geophysics, 61, 373-386, 1996.

Ivan, M., Optimum expression for computation of the magnetic field of a homogeneous polyhedral body, Geophysical Prospecting, 44, 279-288, 1996.

Li, Y., and D.W. Oldenburg, 3D inversion of magnetic data, Geophysics, 61, 394-408, 1996.

Moridis, G.J., L. Myer, P. Persoff, S. Finsterle, J.A. Apps, D. Vasco, S. Muller, P. Yen, P. Williams, B. Freifeld, and K. Pruess, First-Level Field Demonstration of Subsurface Barrier Technology Using Viscous Liquids, LBL Report No. 37520, Lawrence Berkeley National Laboratory, July 1995.

Moskowitz, R., Dynamic sealing with magnetic fluids, ASLE Transactions, 18(2), 135-143, 1975.

Newbower, R.S., A new technique for circulatory measurements employing magnetic fluid tracers, in Proceedings, 1972 Biomedical Symp., San Diego, 1972.

Raj, K, and R. Moskowitz, Commercial applications of ferrofluids, Journal of Magnetism and Magnetic Materials, 85, 233-245, 1990.

Rosensweig, R.E., Fluid dynamics and science of magnetic liquids, In: L. Marton (ed.), Advances in Electronics and Electron Physics, Vol. 48, Academic Press, New York, pp. 103-199, 1979.

Rosenweig, R.E., Ferrohydrodynamics, Cambridge University Press, 1985.

Senyei, A.E., and K. Widder, Drug targeting: Magnetically responsive albumin microspheres - A review of the system to date, Gynecology and Oncology, 12(1), 21-33, 1981.

Shenkel, C.J., Modeling and detection of magnetized proppant in a hydraulic fracture, M.S. Thesis, University of California, Berkeley, 1986.

Telford, W.M., L.P. Geldart, and R.E. Sheriff, Applied Geophysics, 2nd Edition, Cambridge University Press, 1990.

5. Acknowledgements

This work was supported by the Laboratory Directed Research and Development Program of Lawrence Berkeley National Laboratory under the U.S. Department of Energy, Contract No. DE-AC03-76SF00098. Drs. Karsten Pruess and Chao Shan are thanked for their insightful review comments.

Ernest Orlando Lawrence Berkeley National Laboratory
One Cyclotron Road | Berkeley, California 94720

Prepared for the U.S. Department of Energy under Contract No. DE-AC03-76SF00098